Model-Based Feedforward Optimal Control applied to a Turbulent Separated Flow

Maxime Feingesicht, Andrey Polyakov, Franck Kerhervé, Jean-Pierre Richard

Model-Based Feedforward Optimal Control applied to a Turbulent Separated Flow

Maxime Feingesicht [*,**,***] **Andrey Polyakov** [*,**]
Franck Kerhervé [****] **Jean-Pierre Richard** [*,**,***]

[*] *Inria Lille Nord Europe, Parc scientifique de la Haute Borne, 40 Avenue du Halley Bat. A, Park Plaza, 59650 Villeneuve-d'Ascq, France*
[**] *CRIStAL UMR CNRS 9189, Université Lille 1, M3, Avenue Carl Gauss, 59650 Villeneuve-d'Ascq, France*
[***] *Centrale Lille, Cité Scientifique, 59651 Villeneuve-d'Ascq, France*
[****] *Institut P', CNRS UPR 3346, Université de Poitiers, 11 Boulevard Marie et Pierre Curie, BP 30179, F86962 Futuroscope Chasseneuil Cedex*

Abstract: The paper presents a model-based optimal feedforward control methodology applied to the control of a separated flow. A model is first identified as a delayed bilinear model from experimental data using a special identification procedure, for which the precision is compared to other existing results. Then, using the identified model, the optimal feedforward control problem is formulated and solved for the case of a periodic relay control. The theoretical control results are supported with numerical simulations.

Keywords: Bilinear Systems; Time-Delay; Flow Control; Nonlinear Control

1. INTRODUCTION

In the recent years, the transportation industry has become more and more important whether it is for transportation of goods or people. As this requires more frequent travels and higher speeds, the costs tend to rise. One of the main cause of these costs is the aerodynamic loss, also called drag. Reducing this loss is therefore of great economical and ecological interest. Indeed, it will lead to a reduction of the quantity of gas consumed among other benefits. For many years the main way to reduce the drag was shape optimization of the vehicles in order to reduce or suppress part of the turbulent behavior of the flow. This method acts as a passive control but has come close to its maximum efficiency and cannot be applied to most of the already built vehicles. This lead to an increase in the interest for active control strategies (see Brunton and Noack (2015), Chun and Sung (1996), Selby et al. (1992)) as it gives an adaptative and possibly robust method for drag reduction.

In the case of active control, the actuation is often done using air blowers (see, e.g. Volino (2003), McManus et al. (1994), Eldredge and Bons (2004)). The two-dimensional flap (see Raibaudo et al. (2013), Raibaudo et al. (2014), Chabert et al. (2014b), Chabert et al. (2014a), Shaqarin et al. (2013),Chun and Sung (1996), Selby et al. (1992), Cierpka et al. (2007), Ciobaca and Wild (2013) and Åkervik et al. (2008)) constitutes one of the standard benchmark of separated flow control system, extensively studied in the literature and will be considered in the present paper as a test case for the developped methods.

When trying to design a control for tuburlent flows, the first difficulty encountered is the highly nonlinear behavior of the physics involved in the plant. For flows, the governing equations are that given by the partial differential Navier-Stokes equations. In the case of PDEs, the design of a controller based on these equations is excessively complicated because enormous computational power is required due to their infinite dimensions. Their implementation in real-time is almost impossible (see Wachsmuth (2006), Ghattas and Bark (1997), Fernández-Cara et al. (2004)). Multiple control strategies have then been developped to counter this problem, but mostly use linear models (ignoring or linearizing the nonlinear dynamics) and often only deal with feedforward control (see Chun and Sung (1996), Selby et al. (1992), Cierpka et al. (2007), Ciobaca and Wild (2013) and Åkervik et al. (2008)). Among others, recent developments in model-free techniques led to controllers based on machine learning techniques and showed promising results (see Duriez et al. (2016)). However, machine learning requires numerous experiments before being efficient and the reliability and convergence of the algorithms are not well proven. A recent survey of various flow control methods can be found in Brunton and Noack (2015). Model-based robust control of separated flows remains of particular interest and can be implemented in real system without too much complexity if the model is chosen to be sufficiently simple. One of the objectives of the present paper is to study new perspectives in this topic, more precisely focusing on identification and feedforward control.

When aiming at designing a control law to be implemented on an experimental setup, it is necessary for it to be sufficiently simple. In this paper, the model is chosen to be

identified using a modified "grey-box" method such that the model remains simple and with a small number of parameters describing precisely enough the input-output behavior of the flow control system. Furthermore, the control of the considered system is a relay ("ON"/"OFF") actuation provided by pulsed jets (air blowers). Preliminary can be found in Feingesicht et al. (2016).

The present paper focuses on model identification and open-loop control applied to a separated turbulent boundary layer over a flap. The model of the flow is first identified as a bilinear time-delay system and the precision of the model is measured using multiple indicators. Then, an optimal feedforward (open-loop) control is designed based on averaging analysis and given explicitely in the case of relay input. Despite of the fact that bilinear systems were considered in literature (see, e.g. Gauthier and Kupka (1992)), to the best of our knowledge, the considered control problems for bilinear models with state and input delays has never been studied before.

Notation:

- $\mathbb{R}$ is the set of real numbers, $\mathbb{R}_+ = \{x \in \mathbb{R} \mid x \geq 0\}$;
- $\mathbf{C}_\Omega$ is the space of continuous functions;
- $\mathbf{C}_\Omega^{\text{const}}$ be the set of constant-valued continuous functions, i.e. $\xi \in \mathbf{C}_\Omega^{\text{const}}$ if $\xi(s) \equiv$const, $\forall s \in \Omega$;
- $\mathbb{1} \in \mathbf{C}_\Omega$ is the unit constant function: $\mathbb{1}(s) = 1$, $\forall s \in \Omega$;
- $\mathbf{L}^2_\Omega$ is the space of quadratically integrable functions, $\|z\|_{\mathbf{L}^2_\Omega} = \sqrt{\int_\Omega z^2(s)ds}$;
- $\mathbf{L}^\infty_\Omega$ is the space of locally measurable essentially bounded functions, $\|z\|_{L^\infty} = \operatorname*{ess\,sup}_{s\in\Omega} |z(s)|$;
- if $\tau > 0$, $y \in \mathbf{L}^\infty_{\mathbb{R}}$ and $t \in \mathbb{R}$ then $\xi_\tau(t) \in \mathbf{L}^\infty_{[-\tau,0]}$: $(y_\tau(t))(\sigma) = y(t+\sigma)$ for $\sigma \in [-\tau, 0]$. The notation $y_\tau(t)$ and $y_{-\tau}(t)$ is commonly used for time-delay models (see Fridman (2014)).

2. FLOW CONTROL SYSTEM

2.1 Flow Control Problem

The problem of flow control is the meeting point of several research areas (see Brunton and Noack (2015)) :

(1) Fluid Mechanics (for analysis of flow dynamics),
(2) Electronics (for sensing and actuation developments),
(3) Control Theory and Optimization (for formulation of control goals and designing of control laws).

Flow control experimental setup are generally designed and assembled based on current technological achievements in the field of fluid dynamics and electrical engineering. In such a context, the operator cannot have any impact on the set-up, except on the control parameters which drive the actuators. The problem resulting is therefore to optimize efficiency and robustness of the controller by designing appropriate control algorithms.

To the best of our knowledge, the paper presents the first attempts in the context of non-linear (in particular, bilinear) SISO model-based control design for separated flows. This paper deals with the problem of the design of an optimal open-loop (feedforward) control.

2.2 Experimental test case

The experimental test case considered is that of a turbulent boundary layer flow occurring separation along a two-dimensional ramp whose geometry and dimensions are illustrated in Fig. 1. Full details of the experiments, which were conducted in the large boundary-layer wind tunnnel at Laboratoire de Mécanique de Lille (France) can be found in Raibaudo et al. (2015), Raibaudo (2015). The boundary layer flow first develops along a flat horizontal plate (floor of the wind-tunnel) before reaching a smooth convergent where it occurs acceleration. The flow continues to develop along a slightly inclined flat plate to recover a zero pressure streamwise gradient. This is followed by a flap along which the boundary layer occurs separation and reattaches further downstream to the floor of the wind-tunnel. This is illustrated in Fig. 2 where streamlines for the averaged natural flow are reported. Note that the flow comes from the left of the figure. The ramp geometry is shown as the thick black line. In the present configuration, the location where the flow separates from the wall is fixed and located at the edge between the inclined flat plate and the flap (chosen as origin of the coordinate system in figure Fig. 2 and 3). Just downstream of the edge, a shear layer forms and a recirculation region (reversed flow) appears along the flap due to flow separation. The border between positive and negative streamwise mean velocity is represented as the blue line. Below this blue line, the flow is, in average, reversed compared to the flow above the line. The flow in this separation region constitutes the physical system of interest and to control, the main objective of the control being to reduce the recirculation region.

An array of 22 co-rotating round jets, air blowers, aligned parallel to the flap edge is used as actuators. The control input $u(t)$ is a relay ("on"/"off") signal sent to the actuators with a given frequency and duty cycle. An example of the averaged flow obtained when using continuous actuation (relay remains "ON") is illustrated in Fig. 3. Compared to the natural flow discussed previously and shown in Fig. 2, the region of reversed flow is drastically reduced and the flow is found to be almost fully attached to the bottom wall.

For real-time survey, hot-film sensors located along the flap are used to measure the gain in skin friction: an increase in friction gain is representative of flow reattachement. In the present configuration, output voltages of hot-film

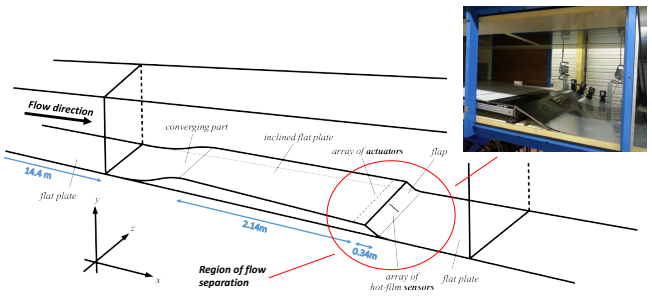

Fig. 1. Diagram and photo of the experimental setup Courtesy of Laboratoire de Mécanique de Lille

sensors are the only signals that can be measured on-line and utilized for control proposes. The output voltages of the sensors are constants in the steady state. The output of the system (value of one of the hot-films voltage ouput or some function of all the hot-films voltages outputs) will be denoted $y(t)$.

2.3 Control Aims

Optimal Control Let us consider the cost functional

$$J(y,u) = \lim_{T\to+\infty} \frac{1}{T}\int_0^T \alpha y(s) - (1-\alpha)u(s)ds \qquad (1)$$

with $0 \leq \alpha \leq 1$, which characterizes the averaged value of y in the steady state and the averaged control value required to obtain it. Since increasing of the output y implies better reduction of turbulence (see Raibaudo et al. (2013)) and since our objective is to reattach the flow as much as possible, we also study the problem of designing a control law u such that

$$J(y,u) \to \max. \qquad (2)$$

The trade-off between the turbulence reduction and the energy consumed by the actuation is provided by the choice of the parameter α.

3. MODELLING AND OPTIMAL CONTROL

3.1 Experimental Data and Pre-Processing

The only data we can use for modeling are the input signals to the actuators and the output voltages of the hot-film sensors measured with a frequency of $1kHz$. Therefore, we cannot design model separately for actuator, sensor and plant, but our model will implicitly include them all.

Several experiments have been done in order to collect an experimental database appropriate for model design.

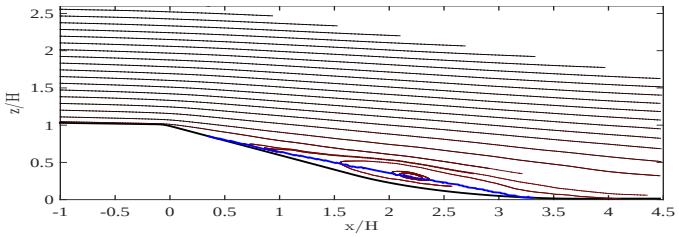

Fig. 2. Streamlines for the flow under continuous actuation

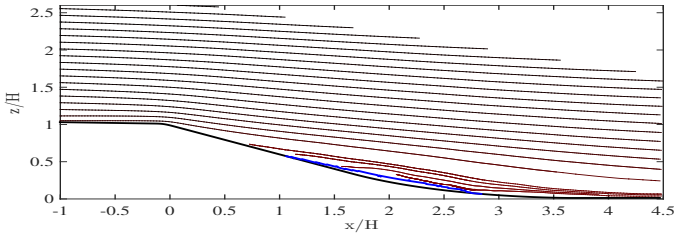

Fig. 3. Streamlines for the natural flow without control. The blue line represents the border between the reversed flow (negative streamwise velocity, region of the flow below the line) and the freestream (positive streamwise velocity, region of the flow above the line). In the controlled case Fig. 3 the recirculation region is shown to be drastically reduced and the flow almost fully reattached to the wall.

Each experiment consists of two phases: actuation and relaxation. Actuation is done by means of a periodic on/off input signal u with a fixed frequency and duty circle (DC). Actuation time is 5 seconds. Seven different input signals have been tested, see Table 1.

During the relaxation phase the control is switched off for 5 seconds in order to let the flow to return to a natural steady separated state. Each experiment is repeated for more than 50 times and the results are phase averaged in order to obtain an output signal less effected by measurement noises and exogenous perturbations. This phase-averaged data (see, Fig. 4) is utilized for modeling.

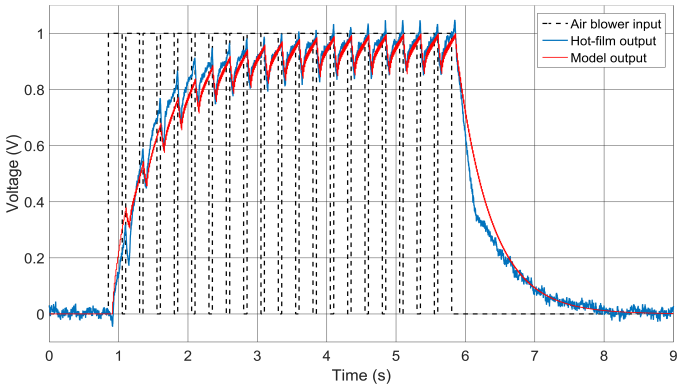

Fig. 4. Phase-averaged data for Freq=4Hz, DC=80%

3.2 Bilinear Model

The dynamics of the flow considered here are highly nonlinear and governed by partial differential equations (e.g. Navier-Stokes equations). The only SISO (Single Input Single Output) model can be designed using the experimental dataset. However, this model should take into account nonlinearity and infinite dimensional nature of the control system. That is why we identify an appropriate model from the class of bilinear control systems governed by differential equations with time delays (i.e. differential-difference equations).

$$\dot{y}(t) = \sum_{i=1}^{N_1} a_i y(t-\tau_i) + \sum_{k=1}^{N_2}\left(b_k + \sum_{j=1}^{N_3} c_{jk} y(t-\tilde{\tau}_j)\right) u_i(t-h_k), \quad (3)$$

where N_1, N_2, N_3 are nonnegative integers, $a_i, b_i, c_{ij} \in \mathbb{R}$ are constant parameters, and both state $\tau_i, \tilde{\tau}_j$ and input delays h_i are considered in order to capture as much as possible the infinite dimensional dynamics of the system. However, this model is sufficiently simple and of small order to design some practically implementable control laws.

Table 1. Input signals used for identification

Test number	Frequency (Hz)	DC
1	Constant	
2	4	50
3	4	80
4	8	50
5	8	80
6	80	50
7	80	80

The identification has been done using a least-square method supported with global optimization algorithm NOMAD (see, Audet et al. (2009); Le Digabel (2011); Audet et al. (2007); Audet and Dennis (2006)) required for optimal assignment of delays. The reader can refer to Feingesicht et al. (2016) for more details about identification of the considered bilinear model.

3.3 Results of Identification

The bilinear models have been identified for $N_1 = N_2 = 2$ and $N_3 = 1$ or 2. The precision of the models has been analyzed using the three indicators : ϵ is L_2-norm of the error, FIT index introduced in Dandois et al. (2013) and ρ - the correlation between the experimental data and the identified model.

$$\epsilon = \|y_{exp} - y_{sim}\|_{\mathbf{L}^2}, \quad \rho = \frac{\mathrm{cov}(y_{exp}, y_{sim})}{\sigma_{y_{exp}}\sigma_{y_{sim}}},$$

$$\mathrm{FIT} = \left(1 - \frac{\|y_{exp} - y_{sim}\|_{\mathbf{L}^2}}{\|y_{exp} - \bar{y}_{exp}\|_{\mathbf{L}^2}}\right) \times 100\%,$$

where y_{exp} is the output of the system obtained from the experiment, y_{sim} is the output generated by the identified bilinear model (3), $\bar{y}_{exp}$ is the mean value of y^{exp}, $\mathrm{cov}\,(y_{exp}, y_{sim})$ is the covariance of y_{exp} and y_{sim}, but $\sigma_{y_{exp}}$ and $\sigma_{y_{sim}}$ are standard deviations of y_{exp} and y_{sim}, respectively. The results are summarized in Tables 2 and 3.

Table 2. Identified parameters of the models

	$N_3 = 1$	$N_3 = 2$
τ_i	$\big[0.054; 0.006\big]$	$\big[0; 0.116\big]$
$\bar{\tau}_j$	$\big[0.054; 0.360\big]$	$\big[0.036; 0.001\big]$
h_k	0.054	$\big[0.045; 0.315\big]$
a_i	$\big[9.5122; -12.5188\big]$	$\big[-11.7146; 7.9658\big]$
b_k	3.5515	$\big[4.4759; 0.3652\big]$
c_{jk}	$\big[-2.2430; 2.2430\big]$	$\big[29.1680; -28.7925; -24.1864; 23.4018\big]$

Table 3. Precision of the identified models

	ε	FIT	ρ
$N_3 = 1$	0.4498	87.11%	0.9918
$N_3 = 2$	0.2987	91.44%	0.9965

Its is worth stressing that the obtained models have very high precision comparing with the existing results Dandois et al. (2013). The FIT index is improved for almost 30% using the model with only 8 parameters (see, Table I). The NARX model obtained in Dandois et al. (2013) has hundreds of coefficients and FIT=59%.

3.4 Model Description and Basic Assumptions

Let us consider the functional differential equation

$$\dot{y}(t) = A(y_\tau(t)) + \sum_{i=1}^{N_3}(b_i + B_i(y_\tau(t - h_i)))u(t - h_i), \quad (4)$$

where $y_\tau(t) \in \mathbf{C}^1_{[-\tau,0]}$ is the state of the system, $(y_\tau(t))(s) = y(t + s)$ for $s \in [-\tau, 0]$, $A : \mathbf{C}^1_{[-\tau,0]} \subset \mathbf{L}^2_{[-\tau,0]} \to \mathbb{R}$ and $B_i : \mathbf{C}^1_{[-\tau,0]} \subset \mathbf{L}^2_{[-\tau,0]} \to \mathbb{R}$ are linear continuous functionals, $b_i \in \mathbb{R}_+$ are positive constants, $u(t) \in \{0, 1\}$ is the relay control input, $h_i \in \mathbb{R}_+$ are input delays. For any $u \in \mathbf{L}^\infty_{\mathbb{R}_+}$ the considered system has a unique Caratheodory solution Hale (1971). Similarly to the previous section we assume that *the system* (4) *with* $y(s) = 0$ *for all* $s \le 0$ *has bounded positive solution for any input signal* $u \in \boldsymbol{L}^\infty_{\mathbb{R}_+} : u(t) \in \{0, 1\}$. We also assume that *the class of admissible control inputs is restricted to* ω*-periodic functions* $u(t) = u(t + \omega)$, $\forall t > 0$.

3.5 Periodic Feedforward Control

In the periodic case, the optimization problem $J(y, u) \to \max$ subject to (4) considered over infinite interval of time can be reduced to the optimal control over finite time interval. Indeed, if for any ω-periodic input $u \in \mathbf{L}^\infty_{\mathbb{R}_+}$ the system (4) has a unique stable ω-periodic solution y^ω then

$$J(y^\omega, u) = \frac{1}{\omega}\int_0^\omega \alpha y^\omega(s) - (1 - \alpha)u(s)ds. \quad (5)$$

To solve this optimization problem we need a proper algorithm of finding of periodic solutions to the system (4) with a given periodic control input u. Existence of periodic solution to a particular system (4) as well as algorithm for its finding is provided by the next theorem.

Theorem 1. (Polyakova (2006)). *If* $0 = h_0 < h_1 < ... < h_m$ *and*

- *a function* $f : \mathbb{R}_+ \times \mathbb{R}^{n(m+1)} \to \mathbb{R}$ *is measurable and* ω*-periodic:* $f(t, \boldsymbol{x}) = f(t + \omega, \boldsymbol{x})$, $t \in \mathbb{R}_+$, $\boldsymbol{x} \in \mathbb{R}^{n(m+1)}$, *and satisfies Lipschitz condition:*
$$|f(t, \boldsymbol{x}) - f(t, \boldsymbol{y})| \le \sum_{i=0}^{n-1}\sum_{j=0}^{m} l_{ij}|x_{ij} - y_{ij}|, \ \boldsymbol{x}, \boldsymbol{y} \in \mathbb{R}^{n(m+1)},$$
where $l_{ij} \ge 0$ *are constants,* $\boldsymbol{x} = (x_{00}, x_{01}, ..., x_{ij}, ...) \in \mathbb{R}^{n(m+1)}$ *and* $\boldsymbol{y} = (y_{00}, y_{01}, ..., y_{ij}, ...) \in \mathbb{R}^{n(m+1)}$,
- *a liner functional* $\mathcal{A} : \boldsymbol{C}^n_{[-h_m,0]} \to \mathbb{R}$ *is defined as*
$$\mathcal{A}x_{h_m}(t) = \sum_{i=0}^{m}\sum_{j=0}^{n} a_{ij}x^{(j)}(t - h_i), \quad a_{ij} \in \mathbb{R},$$
$$x_{h_m}(t) = x(t + s) \text{ for } s \in [-h_m, 0],$$
- *the frequency* $\theta = \frac{2\pi}{\omega}$ *satisfies the non-resonance conditions:* $L\,(\mathrm{i}k\theta) \ne 0$ *for* $k = 0, \pm1, \pm2, ...$ *where* $p = 0, 1, ..., n - 1$ *and* $L(\lambda) = \sum_{i=0}^{m}\sum_{j=0}^{n} a_{ij}\lambda^j e^{-h_i\lambda}$ *is the characteristic quasi-polynomial of the operator* $\mathcal{A}$,
- *the inequality* $q = \sum_{p=0}^{n-1} l_p\sigma_p < 1$ *holds for* $l_p = l_{p0} + l_{p1} + ... + l_{pm}$ *and* $\sigma_p = \max\limits_{r\in\mathbb{R}}\left|\frac{(ir\theta)^p}{L(ir\theta)}\right|$,

then the equation $\mathcal{A}x_{h_m}(t) = f(t, x(t), x(t - h_1), ..., x^{(n-1)}(t - h_m))$ *has a unique* ω*-periodic solution* $x_\omega \in \boldsymbol{C}_{[0,\omega]}$, *which satisfies the estimate* $\|x^{(i)}_\omega\|_{\boldsymbol{L}^2_{[0,\omega]}} \le \frac{\sigma_i}{1-q}\|f(t, \boldsymbol{0})\|_{\boldsymbol{L}^2_{[0,\omega]}}$, $i = 0, 1, ..., n - 1$ *and can be found by means of iterations*

$$\mathcal{A}x^{[k+1]}_{h_m}(t) = f(t, \boldsymbol{x}^{[k]}(t)), k = 0, 1, 2, ..., \quad (6)$$

where $x^{[0]}$ *is an arbitrary* ω*-periodic function and* $\boldsymbol{x}^{[k]}(t) = (x^{[k]}(t), x^{[k]}(t - h_1), ..., x^{[k]}(t - h_m), ...) \in \mathbb{R}^{n(m+1)}$ *and the following estimate*

$$\left\|\frac{d^i x^{[k]}}{dt^i} - \frac{d^i x_\omega}{dt^i}\right\|_{\boldsymbol{L}^2_{[0,\omega]}} \le \frac{q^k}{1-q}\sigma_i\sum_{p=0}^{n-1} l_p\left\|\frac{d^p x^{[0]}}{dt^p} - \frac{d^p x_\omega}{dt^p}\right\|_{\boldsymbol{L}^2_{[0,\omega]}} \quad (7)$$

holds for $i = 0, 1, 2, ..., n-1$.

To the best of our knowledge, the proof of Theorem 1 for $\mathbf{L}^2$ spaces has never been presented in English literature. Its proof given originally in Polyakova (2006).

The formula (6) provides simple recursive procedure for numerical finding of periodic solution with precision controlled by the formula (7). Combination of this algorithm with some infinite dimensional optimization procedure Kantorovich and Akilov (1982) allows us to find numerically an optimal input signal u for a fixed period ω. The corresponding algorithms are usually computationally hard. That is why, for practice, it is also important to provide a simple suboptimal algorithm. One has the following proposition.

Proposition 1. If for any ω-periodic input signal $u \in \boldsymbol{L}^\infty_{\mathbb{R}}$ the poitive system (4) *has a unique globally asymptotically stable periodic solution and* $A(\mathbb{1})+\omega^{-1}\int_0^\omega B(\bar{u}_\tau(s))ds < 0$, *then,*

$$J(y,u) \geq \tilde{J}(u)$$

$$\tilde{J}(u) = \left(\alpha - 1 - \frac{\alpha b}{A(\mathbb{1})+\omega^{-1}\int_0^\omega B(\bar{u}_\tau(s))ds}\right)\omega^{-1}\int_0^\omega u(s)ds$$

where $B(\xi) = \sum_{i=1}^{N_2} B_i(\xi)$ *for* $\xi \in \boldsymbol{L}^\infty_{\mathbb{R}}$ *and* $b = \sum_{i=1}^{N_2} b_i$.

Therefore, if conditions of Proposition 1 holds then the sub-optimal control can be found by means of maximization of the functional $\tilde{J}(u)$.

If periodic control inputs are restricted to

$$u_{\omega,t'}(t) = \begin{cases} 1 & \text{for } t \in [k\omega, k\omega + t'), \\ 0 & \text{for } t \in [k\omega + t', (k+1)\omega), \end{cases} \tag{8}$$

then, in the view of Proposition 1, a quasi optimal solution to (2) can be found from the finite dimensional optimization problem: $\tilde{J}(u_{\omega,t'}) \to \max$. Such class of input signals is motivated by natural practical demands to minimize the number of switchings.

In this case, the condition $A(\mathbb{1}) + \omega^{-1}\int_0^\omega B(\bar{u}_\tau(s))ds < 0$ of 1 simplifies to $A(\mathbb{1}) + \frac{t'}{\omega}B(\mathbb{1}) < 0$, and $\tilde{J}(u)$ to :

$$\tilde{J}(u) = \left(\alpha - 1 - \frac{\alpha b}{A(\mathbb{1})+\frac{t'}{\omega}B(\mathbb{1})}\right)\frac{t'}{\omega} \tag{9}$$

This optimization problem can be solved analytically for $\tilde{J}$. For any fixed value ω_0 of ω, the value of t' noted by t'_0 is given by :

$$t'_0 = \begin{cases} 0 & \text{if } \alpha = 0 \\ \omega & \text{if } \alpha = 1 \\ \omega\ \mathrm{sat}_{[0,1]}\left(-\frac{A(\mathbb{1})}{B(\mathbb{1})} - \frac{\sqrt{\frac{\alpha}{(\alpha-1)}A(\mathbb{1})b}}{B(\mathbb{1})}\right) & \text{if } 0 < \alpha < 1 \end{cases} \tag{10}$$

where $\mathrm{sat}_{[0,1]}$ is the saturation function on the interval $[0,1]$ such that $\mathrm{sat}_{[0,1]}(x) = x$ for $0 \leq x \leq 1$, $\mathrm{sat}_{[0,1]}(x) = 1$ for $x > 1$ and $\mathrm{sat}_{[0,1]}(x) = 0$ for $x < 0$

It is worth stressing that the identified model of the flow control system (see, Table I) satisfies Proposition 1.

3.6 Numerical simulation results

Let us find the suboptimal feedforward control of the form (8) for our system with two input delays as presented in Section 3.5. It is easy to compute that $A(\mathbb{1}) = -3.7488 < 0$ and $A(\mathbb{1}) + B(\mathbb{1}) = -4.1578 < 0$, then the conditions of Proposition 1 are fulfilled for every couple (ω, t').

A numerical simulation can be found in Fig. 5. This simulation was done for $\alpha = 0.47$ and $\omega = 0.25$, leading to $t' = 0.1607$ and the duty cycle $\frac{t'}{\omega} \times 100\% = 64.28\%$.

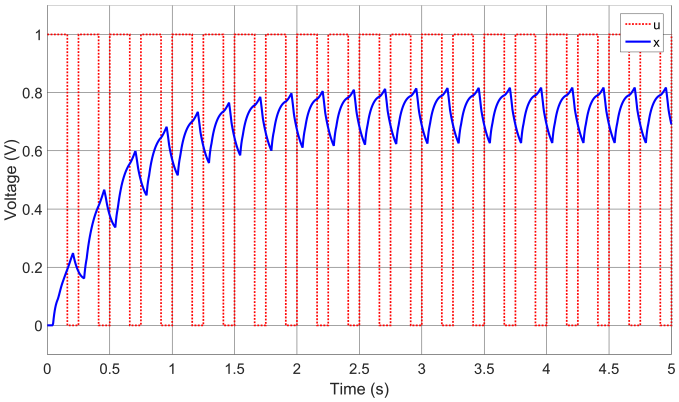

Fig. 5. Application of the feedforward control

4. DISCUSSION AND CONCLUSIONS

This paper considers the problem of identification and model-based open-loop control design for turbulent flows. The model is formulated in a generic way as a bilinear time-delay system, introduced in Feingesicht et al. (2016), in order to capture the nonlinear and infinite dimensional properties of the flow. The model is identified based on experimental data using a specific identification method. Then, averaging analysis is used to analyze this model and deduce an optimal open-loop relay control aimed at maximizing the reattachment of the flow to the wall.

The proposed control was tested in the ONERA Lille wind tunnel. A video of the experiment can be found at : `youtu.be/BLG5e9obQK0`

ACKNOWLEDGEMENTS

This work was carried out within the framework of the CNRS Research Federation on Ground Transports and Mobility, in articulation with the ELSAT2020 project supported by the European Community, the French Ministry of Higher Education and Research, the Hauts de France Regional Council. The authors gratefully acknowledge the support of these institutions.

REFERENCES

Åkervik, E., Hoepffner, J., Ehrenstein, U., and Henningson, D.S. (2008). Model reduction and control of a cavity-driven separated boundary layer. In *IUTAM Symposium on Flow Control and MEMS*, 147–155. Springer.

Audet, C. and Dennis, J. (2006). Mesh Adaptive Direct Search Algorithms for Constrained Optimization. *SIAM*

Journal on Optimization, 17(1), 188–217. doi:10.1137/040603371.

Audet, C., Béchard, V., and Digabel, S.L. (2007). Nonsmooth optimization through Mesh Adaptive Direct Search and Variable Neighborhood Search. *Journal of Global Optimization*, 41(2), 299–318. doi:10.1007/s10898-007-9234-1.

Audet, C., Jr, J.E.D., and Digabel, S.L. (2009). Globalization strategies for Mesh Adaptive Direct Search. *Computational Optimization and Applications*, 46(2), 193–215. doi:10.1007/s10589-009-9266-1.

Brunton, S.L. and Noack, B.R. (2015). Closed-Loop Turbulence Control: Progress and Challenges. *Applied Mechanics Reviews*, 67(5), 050801–050801. doi:10.1115/1.4031175. URL `http://dx.doi.org/10.1115/1.4031175`.

Chabert, T., Dandois, J., and Garnier, É. (2014a). Experimental closed-loop control of flow separation over a plain flap using slope seeking. *Experiments in Fluids*, 55(8), 1–19.

Chabert, T., Dandois, J., Garnier, É., and Jacquin, L. (2014b). Experimental detection of flow separation over a plain flap by wall shear stress analysis with and without steady blowing. *Comptes Rendus Mécanique*, 342(6), 389–402.

Chun, K.B. and Sung, H.J. (1996). Control of turbulent separated flow over a backward-facing step by local forcing. *Experiments in Fluids*, 21(6), 417–426. doi:10.1007/BF00189044.

Cierpka, C., Weier, T., and Gerbeth, G. (2007). Electromagnetic Control of Separated Flows Using Periodic Excitation with Different Wave Forms. In P.D.R. King (ed.), *Active Flow Control*, number 95 in Notes on Numerical Fluid Mechanics and Multidisciplinary Design (NNFM), 27–41. Springer Berlin Heidelberg.

Ciobaca, V. and Wild, J. (2013). An Overview of Recent DLR Contributions on Active Flow-Separation Control Studies for High-Lift Configurations. *Aerospace Lab*, Issue(2013-06).

Dandois, J., Garnier, E., and Pamart, P.Y. (2013). NARX modelling of unsteady separation control. *Experiments in fluids*, 54(2), 1–17.

Duriez, T., Brunton, S., and Noack, B.R. (2016). *Machine Learning Control – Taming Nonlinear Dynamics and Turbulence*. Springer. Google-Books-ID: CxNuDQAAQBAJ.

Eldredge, R. and Bons, J. (2004). Active Control of a Separating Boundary Layer with Steady Vortex Generating Jets - Detailed Flow Measurements. In *42nd AIAA Aerospace Sciences Meeting and Exhibit*. American Institute of Aeronautics and Astronautics.

Feingesicht, M., Raibaudo, C., Polyakov, A., Kerherve, F., and Richard, J.P. (2016). A bilinear input-output model with state-dependent delay for separated flow control. URL `https://hal.inria.fr/hal-01298166/document`.

Fernández-Cara, E., Guerrero, S., Imanuvilov, O.Y., and Puel, J.P. (2004). Local exact controllability of the Navier–Stokes system. *Journal de Mathématiques Pures et Appliquées*, 83(12), 1501–1542. doi:10.1016/j.matpur.2004.02.010.

Fridman, E. (2014). *Introduction to Time-Delay Systems: Analysis and Control*. Springer.

Gauthier, J.P. and Kupka, I. (1992). A separation principle for bilinear systems with dissipative drift. *IEEE transactions on automatic control*, 37(12), 1970–1974.

Ghattas, O. and Bark, J.H. (1997). Optimal Control of Two- and Three-Dimensional Incompressible Navier–Stokes Flows. *Journal of Computational Physics*, 136(2), 231–244. doi:10.1006/jcph.1997.5744.

Hale, J.K. (1971). Caratheodory Conditions. In *Functional Differential Equations*, number 3 in Applied Mathematical Sciences, 30–31. Springer US. DOI: 10.1007/978-1-4615-9968-5_7.

Kantorovich, L. and Akilov, G. (1982). *Functional Analysis. 1982*. Pergamon Press, Oxford.

Le Digabel, S. (2011). Algorithm 909: NOMAD: Nonlinear optimization with the MADS algorithm. *ACM Transactions on Mathematical Software (TOMS)*, 37(4), 44.

McManus, K., Legner, H., and Davis, S. (1994). Pulsed vortex generator jets for active control of flow separation. American Institute of Aeronautics and Astronautics. doi:10.2514/6.1994-2218. URL `http://arc.aiaa.org/doi/10.2514/6.1994-2218`.

Polyakova, L. (2006). Generalized fixed-point theorems and periodic solutions of non-linear equations.

Raibaudo, C., Polyakov, A., Kerherve, F., Richard, J.P., and Stanislas, M. (2015). Experimental open-loop and closed-loop control of a massive separated boundary layer at high Reynolds number.

Raibaudo, C. (2015). *Characterization of the transient of a separated turbulent boundary layer under control and applications to advanced closed-loop controllers*. Ph.D. thesis, Ecole Centrale de Lille.

Raibaudo, C., Kerherve, F., and Stanislas, M. (2013). Characterisation of the transient dynamics of a controlled separated flow using phase averaged PIV. In *International Conference on Instability and Control of Massively Separated Flows – ICOMASEF*.

Raibaudo, C., Polyakov, A., Efimov, D., Kerherve, F., Richard, J.P., and Stanislas, M. (2014). Experimental closed-loop control of a detached boundary layer at high Reynolds number. In *10th EUROMECH Fluid Mechanics Conference*.

Selby, G.V., Lin, J.C., and Howard, F.G. (1992). Control of low-speed turbulent separated flow using jet vortex generators. *Experiments in Fluids*, 12(6), 394–400. doi:10.1007/BF00193886.

Shaqarin, T., Braud, C., Coudert, S., and Stanislas, M. (2013). Open and closed-loop experiments to identify the separated flow dynamics of a thick turbulent boundary layer. *Experiments in Fluids*, 54(2), 1–22. doi:10.1007/s00348-012-1448-4.

Volino, R.J. (2003). Separation Control on Low-Pressure Turbine Airfoils Using Synthetic Vortex Generator Jets. 845–859. doi:10.1115/GT2003-38729. URL `http://dx.doi.org/10.1115/GT2003-38729`.

Wachsmuth, D. (2006). *Optimal control of the unsteady Navier-Stokes equations*. Ph.D. thesis, PhD thesis, Technische Universität Berlin.